International Journal of Thermofluids 7–8 (2020) 100040

Contents lists available at ScienceDirect

International Journal of Thermofluids

journal homepage: www.elsevier.com/locate/ijtf

Evaluation of waste heat recovery technologies for the cement industry

José J. Fierro[a], Ana Escudero-Atehortua[a], César Nieto-Londoño[*,a], Mauricio Giraldo[b], Hussam Jouhara[c], Luiz C. Wrobel[c]

[a] Escuela de Ingenierías, Universidad Pontificia Bolivariana, Medellín, Colombia
[b] Cementos Argos, Medellín, Colombia
[c] College of Engineering, Design and Physical Sciences, Brunel University London, London, England

ARTICLE INFO

Article History:
Received 29 May 2020
Revised 27 July 2020
Accepted 28 July 2020
Available online 12 August 2020

Keywords:
Clinker kiln
Feed preheating
Organic Rankine Cycle
Waste-heat recovery
Exergo-economic analysis

ABSTRACT

Cement is the world's most widely used construction material. In 2019, global production amounted to 4086 MT, of which Colombia contributed 12.59 MT. The main component of cement is Clinker and it appears as an intermediate product in the manufacturing process that is produced in a kiln system at sintering temperatures. Such a process exhibits high environmental impacts due to both elevated emissions of Carbon Dioxide and fuel consumption and it is inherently prone to thermal inefficiencies, as heat losses to the surroundings, because of the large flow rates and high temperatures. In this work, the waste heat obtained from the cooling of a high-temperature gas effluent from the rotary kiln in a Colombian cement plant is analysed for its potential use either to dry wet raw material (limestone) or to generate electricity through an ORC. Material, energy and exergy balances for the steady-state were assisted with simulations in Aspen Plus V.10 software. Exergo-economics analysis followed the traditional approach using the net present value (*NPV*) of the investment as decision criteria. To achieve a holistic view of the waste heat recovery scenario a sensitivity analysis is carried out varying the outlet temperatures of the hot gases for various working fluids in the ORC. Results showed that the best alternative, *NPV* = 0.37 MUSD at market conditions of electricity and fuel sale price, delivers a maximum of 3.77 MW of electricity with a thermal efficiency of 15.96% and an exergy efficiency of 37.52% using Cyclo-Pentane as working fluid. None of the dryer units attained a positive *NPV* and were discarded. However, the highest moisture reduction in the solids stream was 5.67% at $T = 120\ ^{\circ}C$. The option of placing a drying unit immediately after an ORC to completely cool down the gases was economically analysed for ORC cases with best *NPV*, $T = 150\ ^{\circ}C$ and $T = 180\ ^{\circ}C$. But no substantial improvement was found over using the ORC alone. The possibility to improve the simple ORC performance is explored through the inclusion of an internal heat exchanger, such recuperated cycle outperforms its simpler configuration in terms of thermal and economic performance delivering 4.1 MW of net work with an *NPV* = 0.42 MUSD, a rate of return of 15.58% and a payback time of *PB* = 6.07 years. This is 8.75% more work with 13.51% better economic performance than the simple ORC.

1. Introduction

The production of cement is a complex process that starts with the mining and grinding of raw mineral material, mainly limestone and clay, to a fine homogeneous powder called "Raw Meal". It is then heated up to sintering temperatures in a rotary kiln where a set of chemical reactions and physical transformations occur, generating clinker, that is a granulated intermediate compound, which, once ground to a fine powder and mixed with gypsum, becomes Ordinary Portland Cement (OPC) [1]. The process involves several steps of pre-conditioning, grinding, drying, classifying, heating, and cooling, all of them demanding a certain amount of energy in the forms of electricity and heat. For the reactions to take place, the higher input of energy is in the form of heat from burning of the fuel in the kiln. Such fuel consumption accounts for useful energy as well as for heat losses. A typical energy balance for a modern kiln, reveals that about 23% of the heat is lost with waste gases, 11% with the cooler excess gas and 10% by radiation throughout the entire surface of the system, adding up to an impressive 44% of the total heat input in the traditional dry technology kilns [2]. The impact generated on the environment by the production of cement should be noted since considerable amounts of CO_2 are released into the atmosphere due to the combustion of fuels and to the limestone's decarbonation reaction, that is, around 5% of all man-made CO_2 [3].

* Corresponding author.
E-mail address: cesar.nieto@upb.edu.co (C. Nieto-Londoño).

https://doi.org/10.1016/j.ijft.2020.100040

Nomenclature

Parameter

$\dot{X}$	Exergy rate
$\dot{m}$	Mass flow
h	Enthalpy
T	Temperature
$\dot{W}$	Work
η	Efficiency
$\dot{I}$	Exergy destruction rate
$\dot{Q}$	Heat flow
EDF	Exergy destruction factor
VFR	Volumetric flow ratio
SP	Size parameter
$\dot{C}$	Cost rate
f_k	Exergo-economic factor
$\dot{Z}$	Cost rate of capital or investment costs
Z	Cost of capital or investment costs, present value
c	Average unit cost
CRF	Capital recovery factor
i	Rate of return
NPV	Net present value
PB	Payback time
R_t	Annualised cash-flow

Subscript

f	fluid
i	i^{th} stream
0	dead state
wf	working fluid
s	isentropic
is	isentropic
hs	heat source
cw	cooling water
in	entering
out	exiting
exp	expander
$mech$	mechanical
$cond$	condenser
th	thermal, first law
exg	exergetic, second law
tot	total
ew	evaporated water
exh	exhaust
$mech$	mechanical
t	total
eff	effective
el	electricity

Superscript

CI	Capital Investment
OM	Operation and Maintenance

Abbreviations

IHE	Internal Heat Exchanger
NFPA	US National Fire Protection Association
MUSD	Million dollars

Energy-intensive processes and industries, like iron and steel, petrochemical, cement, pulp and paper, ceramics, glass and food are responsible for 1/3 of annual global greenhouse gas emissions. Because of this, various alternatives are currently being explored, from technical approaches to regulatory modifications with the intention of mitigating the harmful effects, namely, the decarbonisation of low temperature heat by cross-sector technologies, the use of membranes in the petrochemical industry, carbon neutral steel-making, alternative feed-stock for cement production and carbon capture and storage [4,5]. Previously disregarded systems like aluminium production are being solidly addressed for the recovery of waste heat in recent research projects such as ETEKINA and the use of heat pipes has become popular as a cost-effective alternative for these purposes [6,7]. As a general rule, such processes as cement production require both high temperatures ($>1400\,^{\circ}C$) and enormous flow rates, entailing the consumption of large amounts of energy, usually from fossil fuels and electricity [8]. As stated in [9] in 2012 the total estimated primary energy usage was 474171 PJ from which the industrial sector is responsible for about 22% and only around 49% of it ends up being useful. The rest is rejected as waste heat with different qualities according to the available temperature: high quality ($T > 300\,^{\circ}C$) corresponding to 22%, medium quality ($100\,^{\circ}C < T < 300\,^{\circ}C$) 12%, low quality ($T < 100\,^{\circ}C$) 25% and the balance being losses. Consequently, the waste heat potential (energy) varies from 6.00% to 12.60% and the Carnot potential (exergy) from 1.73% to 6.40% [10–12]. It is important to note that coal accounts for 31–42% of the fuel used to meet the energy usage in the cement industry [13] which in turn represents 12.5% of the overall industrial demand for coal (~ 1780 Mtce) [14]. Accordingly, the global production of cement is 4086 MT/y (as shown in Table 1) and it requires a total energy supply of fuel that ranges between 530–728 Mtce.

Such waste energy could be recovered through any of the different approaches listed by [11] as direct heat usage (commonly preheating or drying operations) or in heat to electricity conversion through a power cycle (Rankine, ORC, Kalina, TFC, external combustion engines, etc.). Cement plants present many challenges in terms of energy usage, which is why several attempts have been made to optimise resources and equipment to increase the process efficiency and to reduce costs. However, each case has specific needs as a result of the particular constraints imposed by the previous processes, the infrastructure and the economic conditions of each company. In [12,15] the thermodynamic and exergo-economic analysis of a cement plant in Turkey is shown. First, a general overview of the manufacturing process is provided and the methodology to be followed: raw material preparation and raw grinding; pre-heating, calcination and cooling, final grinding and distribution. Energetic and exergetic relations were summarised for the most common operation units in the plant, as well as, the procedure to estimate costs. Second, actual calculations and analysis were performed indicating a significant potential for increasing exergy efficiency by improving exergy utilisation in the pyroprocessing tower (thermal efficiency of η_{th} = 55.86%), rotary kiln (η_{th} = 52.14%) and clinker cooler. The overall

Table 1
Global cement production statistics for the year 2019* [36].

Country	Production [MT/y]	Share [%]
China	2200	53.84
India	320	7.83
Vietnam	95	2.33
United States**	89	2.18
Egypt	76	1.86
Indonesia	74	1.81
Iran	60	1.47
Russia	57	1.40
Korea, Republic of	55	1.35
Brazil	55	1.35
Japan	54	1.32
Turkey	51	1.25
Colombia***	12.59	0.31
Other countries (rounded)	887	21.72
World total	4086	100

*Estimated **Includes Puerto Rico ***[37]

balance also showed that 71.87MW corresponding to 85.12% of the total energy input is lost through the outer shell of the kiln and the pyroprocessing tower. This indicated that the rotary kiln is by far the most exergy destructive unit in the plant where small improvements can provide better developments in plant performance than large improvements in other components.

An energetic and exergetic optimised Rankine Cycle for waste heat recovery from the chimneys of the Sabzevar cement factory is proposed in [16] to be used in the generation of power to improve the plant energy efficiency. It is found that an increase in the boiler pressure decreased the amount of recovered energy while increasing the cycle efficiency; therefore, there would be an optimum point, found at 1398 kPa, where both the highest overall energy and exergy efficiencies were achieved. Moreover, the effects of important operating parameters such as maximum cycle temperature, environmental temperature, and condenser pressure were investigated showing that boiler optimum pressure is independent and remained constant when these parameters changed. The utilisation of a Kalina cycle for waste heat recovery and electricity generation (2.4MW) from the exhaust gases of the cyclone pre-heater of the rotary kiln in a Brazilian cement plant is assessed by [17]. They showed that reducing the pinch point in the evaporator and increasing the ammonia concentration at its outlet leads to an increase in the delivered net power, while the increase in the turbine inlet pressure decreased the cost of the electricity generated to roughly 0.05$/kWh. The thermal efficiency achieved by the cycle was η_{th} = 23.3% and an exergetic efficiency of η_{exg} = 47.8%.

Heat recovery alternatives such as ORCs have been extensively studied in previous work and some relevant cases are presented below. A parametric optimisation and performance analysis of a waste heat recovery system from a flue gas at T = 140 °C is developed in [18]. R-12, R123 and R134a are considered for evaluation as suitable working fluids. Results showed that R-123 has the maximum work output and efficiencies. The system can generate 19.09 MW at η_{th} = 25.30% which is close to the Carnot efficiency and a η_{exg} = 64.40%. In [19] a thermo-economic optimisation of waste heat recovery by ORC takes place. Several working fluids are considered: R245fa, R123, n-butane, n-pentane, R1234yf and Solkatherm. It is found that, for the same fluid, the objective functions, economic profitability and thermodynamic efficiency, lead to different working conditions in terms of evaporating temperature. The economical optimum is obtained for n-butane with a specific cost of approximately 2320 $/kW, a net output power of 4.2 kW.

In [20] there is a performance comparison and parametric optimisation of sub-critical ORC and trans-critical power cycle for a low temperature (i.e. 80−100 °C) geothermal heat source. Five indicators were used: thermal, exergy and recovery efficiency, heat exchanger area per unit power and the levelized cost of energy (*LCOE*). Results indicate that R123 in a sub-critical ORC system yields the highest thermal and exergy efficiency of η_{th} = 11.1% and η_{th} = 54.1% respectively. Although having lower efficiencies, the trans-critical cycle operating with R125 provides 20.7% larger recovery efficiency and the *LCOE* value is relatively low. It also provides larger savings in petroleum consumption and CO_2 emissions. Therefore, R125 in trans-critical power cycle can maximise utilisation of the geothermal heat source. Meanwhile, in [21] the optimal evaporation temperature and working fluid were estimated for a sub-critical organic cycle. The larger net power output will be produced when the critical temperature of working fluids approaches the temperature of the waste heat source. Despite the analysis relying solely on thermodynamic considerations when based on the screening criteria of the maximum net power output, suitable working pressure, total heat transfer capacity and expander *SP* of ORC, R114, R245fa, R123, R601a, n-pentane, R141b and R113 are suited as working fluids in sub-critical ORC under the given conditions (i.e., heat source at T = 150 °C).

In [22] it is presented a comprehensive estimate of ORC units that can be installed for waste heat recovery in European energy-intensive industries. This study showed that in the most convenient considered scenario (for 2013) up to about 20,000 GWh of thermal energy per year can be recovered and 7.6 Mton of CO_2 can be saved by the application of ORC technology. It was estimated for the cement industry that in the 27 European countries of the study over 576 MW of ORC can be installed whether recovering heat from the pre-heating cyclones or from clinker cooler gases. Thermal efficiency and specific investment cost of basic ORC, single stage regenerative and double stage regenerative ORC have been optimised in [23] through a genetic algorithm approach. The optimisation result shows that R245fa is the best working fluid under the considered conditions. A sensitivity analysis noted that the evaporation pressure has a promising effect on thermal efficiency and specific investment cost. A multi-objective thermo-economic optimisation strategy to assess ORCs is applied by Lecompte et al. [24] to sub-critical and trans-critical cycles for waste heat recovery. The minimum specific investment cost was used as an economic appraisal criterion in a post processing step and it is found that the sub-critical cycle outperforms the trans-critical one. Such a result leads to a lower payback time but not necessarily the highest *NPV*.

In [25] a thorough comparison of a TLC, ORC and Kalina cycles was carried out from the viewpoint of thermodynamics and thermo-economics using a low grade heat source with a temperature of T = 120 °C. Results showed that for the TLC an increase in the expander inlet temperature leads to an increase in net power output and a decrease in product cost for this power plant. However, it was observed that for both, the ORC and Kalina systems, the optimum operating condition for maximum net output power differs from that for the minimal cost. The costing process in this work was accomplished according to [26]. That is, considering the cost rates of the destroyed exergy and using the traditional exergo-economic factor. A comparative assessment of ORC integration for low-temperature (160 °C) geothermal heat source applications appears in [27] and focuses on three different configurations of ORC for which the optimal operating conditions is obtained in terms of specific investment cost and maximum exergy efficiency. R245fa exhibits highest exergy efficiency of 51.3% corresponding to minimum specific cost of 2423 $/kW for basic cycle, 53.74% to 2475$/kW for recuperated, and 55.93% to 2567$/kW for regenerative cycle.

In [28] it is displayed a case study of waste heat recovery from a large diesel engine exhaust in an offshore platform through the implementation of an ORC system using zeotropic mixtures as working fluid. Different configurations of such power cycle are evaluated in terms of exergetic and economic performance and it is found that the highest efficiencies (16.81% energy, 40.75% exergy) are met for the recuperated ORC with a mixture of R236ea/Cyclohexane (with a ratio of 0.6/0.4). However, the lowest specific investment cost for the most cases is achieved at the mass fractions of 0.1 and 0.5 and it is greater for the recuperated ORC. In [29] is depicted a super-heated regenerative ORC system for low-temperature (160 °C) waste heat recovery. Such a system relies on the inclusion

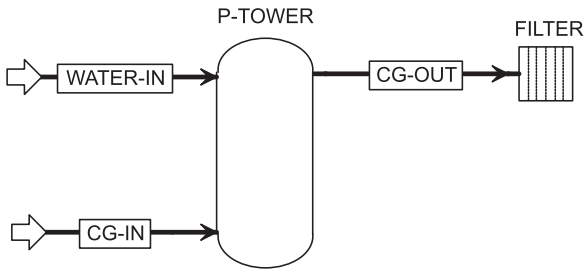

Fig. 1. Pre-conditioning tower schematics.

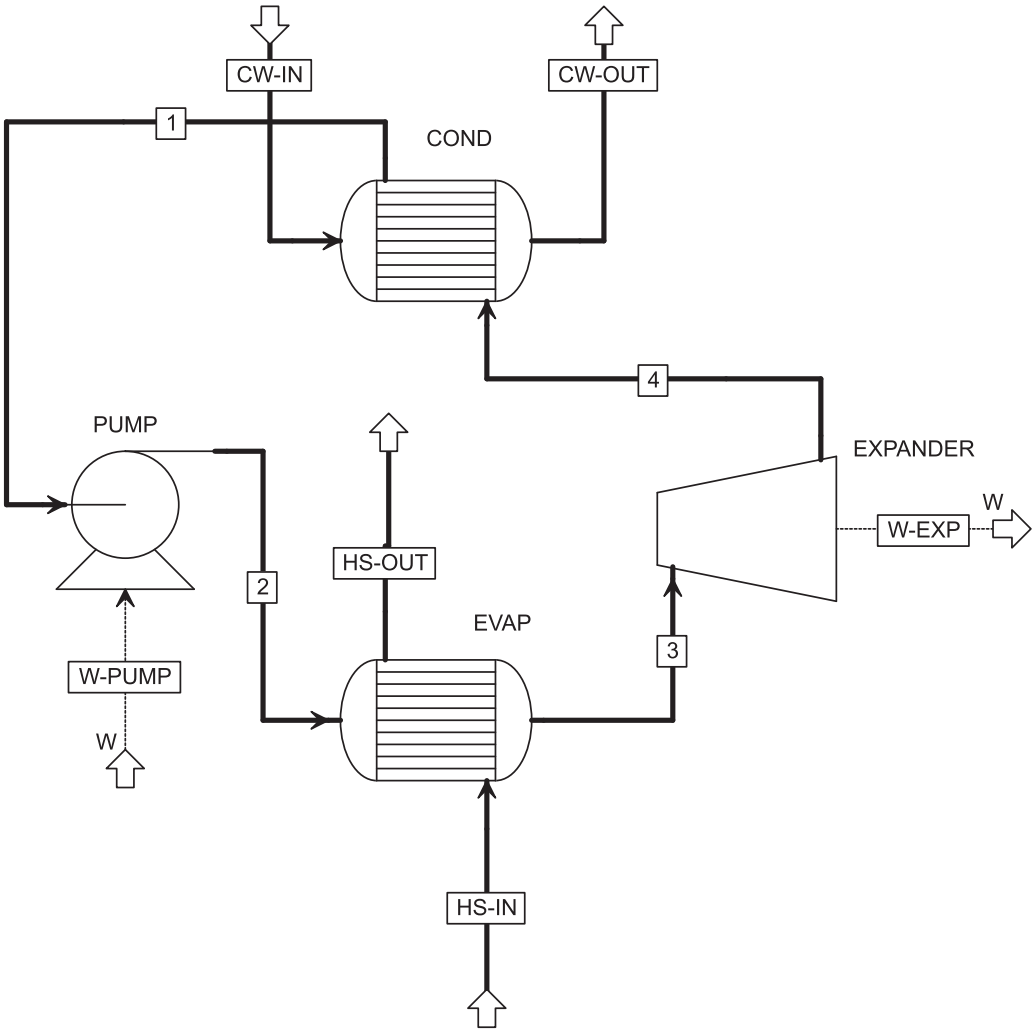

Fig. 2. ORC schematics.

Table 2
Parameters and boundary conditions of the ORC model (base case).

Stream	Parameter	Value	Unit	Ref.	Stream	Parameter	Value	Unit	Ref.
$h_{s,in}$	Temperature	327	°C		3	Temperature	170	°C	
$h_{s,out}$	Temperature	180	°C		4	Vapour fraction	1		
$c_{w,\ in}$	Temperature	27.8	°C			$\eta_{is,exp}$	0.85		[16]
cw,out	Temperature	37.8	°C			$\eta_{mech,exp}$	0.99		[16]
1	Temperature	60	°C			$\eta_{is,pump}$	0.7		[16]

of an Internal Heat Exchanger (*IHE*) to preheat the feed to the evaporator, therefore, increasing the average evaporating temperature while the condensation temperature decreases. It is found that for different working fluids a suitable degree of super-heating is conducive to improving the working capacity and reduces the *VFR*, total capital cost, *SIC*, and *LCOE*. The best comprehensive performance of the cycle is achieved for n-butane with an optimal evaporation temperature of T = 100 °C and a degree of super-heating of 5 °C.

In [30] a thermo-economic optimisation of small-scale ORCs based on screw or piston expanders is found. On this scale, such expanders are said to perform better economically than traditional turbines. The maximum net power output is found to be 17.7 kW. Financial appraisals show a high sensitivity of the investment profitability, though, to the value of the electricity produced and the heat-demand intensity. The optimised case is for an energy cost of 0.14 $/kWh with a payback time of 4 years. A multi-objective thermo-economic optimisation of ORC power systems in waste heat recovery applications is performed by [31] using computer aided molecular design techniques. The optimal working fluids are applied to a sub-critical ORC in different applications spanning a range of heat-source temperatures (T = 150 °C, 250 °C, and 350 °C). When minimising the specific investment cost (*SIC*) of these systems, it is found that the optimal molecular size of the working fluid is linked to the heat-source temperature. Optimal working fluids at the above-mentioned temperatures are propane (*SIC* = 12,326 $/kW), 2-butane (*SIC* = 4919 $/kW) and 2-heptene (*SIC* = 3543 $/kW) respectively. However, when mixed-integer non-linear programming optimisation is applied, for T = 150 °C the best working fluid is 1,3-butadiene (*SIC* = 11,738 $/kW) and for T = 250 °C it is 4-methyl-2-pentene (*SIC* = 4870 $/kW) and such a fluid would not be selected *a priori* in a traditional approach.

In [32] the feasibility to integrate a waste heat recovery ORC system to an unconventional energy-intensive application is evaluated.

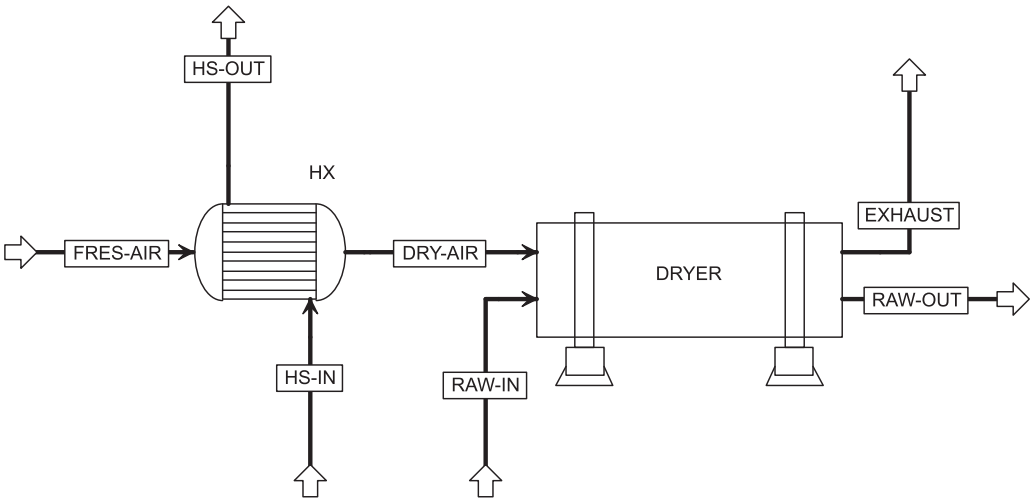

Fig. 3. Drying unit schematics.

Natural gas compressor stations consume large amounts of energy to compensate for pressure losses from individual producing stations to final users and the required power usually comes from the utilisation of multiple gas turbines working at part-load conditions that discharge a significant portion of the primary energy introduced with natural gas into the atmosphere by the exhaust gases as waste heat. Recuperated ORC layouts with intermediate heat exchange fluid and direct heat exchange are assessed and results confirm that by retrofitting the gas turbine units it is possible to generate from 20% and up to 50% of the mechanical energy used by the facility. That is, potential savings of energy and CO_2 equal to 114 GWh/year and $29.6x10^3$ tons/year in the case of RB211 (Rolls Royce commercial ORC) direct heat exchange configuration.

The exergo-economic analysis and optimisation of a new combined power and freshwater system driven by waste heat of a marine diesel engine is presented in [33]. The optimisation relied on a multi-objective genetic algorithm and focuses on the thermal efficiency, exergetic efficiency and the sum of unit costs of products. The values attained for the cogeneration system are 91.84%, 24.33% and 192.7 $/GJ respectively. Cost analyses were carried out as stated in [26]. In [34] a cascade absorption heat transformer is proposed to utilise industrial low grade waste heat. Conventional and advanced exergy and exergo-economic analyses were carried out to determine the cause and avoidable degree of the exergy destruction and cost rates of the components. The analysis shows that only 21.28% of the exergy destruction rates are avoidable by improvement, while 80.2% of the investment cost rates are from the components themselves.

Finally, an exergo-economic analysis of energy utilisation of a drying process in a ceramic production was carried out by [35]. Actual operational data is used in the economic assessment of the spray dryer (η_{th} = 58.79%, η_{exg} = 49.4%), vertical dryer (η_{th} = 51.88%, η_{exg} = 44.96%) and furnace (η_{th} = 36.98%, η_{exg} = 16.41%) for a yearly production capacity of 24 million m^2. Indicators as energy and exergy efficiencies, improvement potential rate, total cost and an exergo-economic factor (the ratio of exergy loss to capital cost rate) are used to understand the overall performance of the system. It is found that in general, the worst performance is of the furnace due to the high temperatures (up to 1250 °C) and large dimensions (85–100 m length) that cause greater exergy destruction and exergy losses to the ambient.

This work focuses on the case study analysis of a cement plant with a kiln capacity of more than 5000 tonnes/day of clinker located at sea level, near the Colombian Atlantic coast. This production plant is one of the largest in the company and an improvement in its efficiency would eventually translate into benefits in the form of competitiveness and responsibility towards the environment due to reduced emissions. The assessment of waste heat recovery potential and the exergo-economic evaluation of different alternatives are pursued to select the one that best suits the current scenario. Initially, the case study is described, with its characteristics and restrictions. Then the relevant energy and exergy balances, as well as cost equations, are presented and finally, the analysis of the results is performed for the ORCs and the raw meal drying system with pertinent conclusions. Accordingly, the generated knowledge and the developed strategy could also be replicated in other plants with similar conditions.

1.1. Case study

A hot effluent current ($T \sim 350$ °C) within a cement production facility was identified, from which to recover waste heat. The plant uses the dry cement production route and it is necessary to dry the crushed raw material (limestone 50–75 mm in size) before it enters to the raw material mill where it is ground to the fine powder known as "Raw Meal". Then, it goes into the rotary kiln at sintering temperatures (> 1400 °C) producing clinker. The kiln has a processing capacity of more than 5000 tonnes/day and coal is used as the main fuel. However, the electrical energy required by the plant is supplied through an internal combustion engine running on diesel.

The exhaust stream of combustion gases from the kiln contains particulate matter that is currently removed in a bag filter. The high temperature damages the filter; therefore, it is necessary to cool down the flow with a water injection as it enters the preconditioning tower. A brief schematic of this process is shown in Fig. 1. The water intake is pulsed rather than constant over time, depending on the operational conditions in the kiln. It is injected into the stream in cases where either the temperature or the gas flow is increasing (i.e, when the raw mill is not using part of the effluen`t from the kiln) to avoid outlet temperatures higher than the desired operational point, T = 180 °C, at which it will not degrade the bag filter materials. In a preliminary analysis, plant data were used to estimate the heat loss due to convection and radiation from the equipment, this was found to be 3.79 MW. The mean temperature of the hot gases once such heat was removed is T = 327 °C. Hence, this temperature is the one that is going to be used as the input in the following sections.

As said before, it is desirable to implement a heat recovery alternative that initially cools down the hot gas stream to dispense with the water injection. At the same time, this would either provide a drier raw material feed to the kiln, via a drying unit, or generate electricity using an ORC to be consumed within the plant or to be sold to the grid. That would benefit the company and stakeholders in the form of competitiveness and responsibility towards the environment

due to reduced emissions. To achieve this, a simulation-based analysis is performed where material, energy, and exergy balances are assisted with Aspen Plus V.10 software and the Aspen Process Economic Analyzer (APEA) assists with the alternative costs. Moreover, the Peng-Robinson equation of state is used to model all gases.

2. Waste heat recovery alternatives

This section specifies the systems identified for heat recovery in the above-mentioned cement plant. Section 2.1 presents the models used to estimate the overall performance of the Organic Rankine Cycle using different working fluids for electricity generation. Then, in Section 2.2 mass, energy and exergy balances for evaluating raw material drying systems are described. Finally, in Section 2.3 exergy models and their corresponding relation with capital and operational costs for each technology are presented.

2.1. Organic Rankine Cycle for electricity generation

The Organic Rankine Cycle (ORC) is perfectly suitable for recovering waste heat in industrial environments [38]. For high-temperature exhausts as the heat source, alkanes are a feasible working fluid [39]; however, the traditional approach in lower temperature applications includes the use of refrigerants [30,40]. Due to the large amount of working fluids that could be used, the criteria proposed by [30] are followed:

- Global warming potential (GWP) $\leq$ 1430 (R134a)
- Ozone depletion potential (ODP) $\leq$ 0.01
- Health (*NFPA*) $\leq$ Moderate hazard (2)
- Instability (*NFPA*) $\leq$ low hazard (1)

Consequently, in this work, four different working fluids: Pentane, Cyclo-Pentane, R134a, and R1234yf, are evaluated in a simple generic configuration of ORC (Fig. 2) to harness the heat from the combustion gases while cooling down the heat source stream.

The parameters and boundary conditions of the ORC model are summarised in Table 2 for a base case where the outlet temperature of the hot gases is set at T = 180 °C. In addition, no pressure losses are considered and the pump's discharge pressure was set at the point of maximum expander work for each working fluid.

The exergy rate, $\dot{X}_i$, of any stream can be expressed as:

$$\dot{X}_i = \dot{m}_f[(h_i - h_0) - T_0(s_i - s_0)], \tag{1}$$

where $\dot{m}_f$ and h are the mass flow and the enthalpy of the stream, respectively, while subscript $_0$ refers to the dead state in which no further interaction between the system and the environment is allowed, thus, no potential for developing work is considered [41]. Eqs. (2) to (9) show a convenient arrangement of the energy and exergy balance equations for each component studied in this work. The total required pumping work $\dot{W}_{pump}$ is calculated using the isentropic efficiency of the pump $\eta_{is,pump}$, as follows,

$$\dot{W}_{pump} = \dot{m}_{wf}(h_{2s} - h_1)/\eta_{is,pump}, \tag{2}$$

while the pump destroyed exergy $\dot{I}_{pump}$ can be expressed in the following way,

$$\dot{I}_{pump} = \left(\dot{X}_1 - \dot{X}_2\right) + \dot{W}_{pump}. \tag{3}$$

Regarding the Evaporator, the heat transfer from the hot gases to the ORC takes place in this unit. The heat input $\dot{Q}_{in}$ is evaluated as,

$$\dot{Q}_{in} = \dot{m}_{hs}(h_{hs,in} - h_{hs,out}), \tag{4}$$

and the destroyed exergy in the evaporator $\dot{I}_{evap}$ is calculated as,

$$\dot{I}_{evap} = \left(\dot{X}_{hs,in} - \dot{X}_{hs,out}\right) - \left(\dot{X}_3 - \dot{X}_2\right). \tag{5}$$

The isentropic, $\eta_{is,exp}$, and mechanical, $\eta_{mech,exp}$, efficiencies of the expander are used to estimate the work delivered $\dot{W}_{exp}$ through the expansion of the working fluid,

$$\dot{W}_{exp} = \dot{m}_{wf}(h_3 - h_{4s})\eta_{is,exp}\eta_{mech,exp}. \tag{6}$$

The destroyed exergy in the expander includes the fluid transport work, as well as the stream inlet and outlet exergies, as follows,

$$\dot{I}_{exp} = \left(\dot{X}_3 - \dot{X}_4\right) - \dot{W}_{exp}. \tag{7}$$

The heat rejected from the cycle to the environment $\dot{Q}_{out}$ at the condenser unit is determined using cooling water as the coolant as advised in [42] for the expected temperatures and an approach of 10 °C,

$$\dot{Q}_{out} = \dot{m}_{cw}(h_{cw,out} - h_{cw,in}), \tag{8}$$

while the exergy destroyed in the condenser $\dot{I}_{cond}$ is evaluated as follows,

$$\dot{I}_{cond} = \left(\dot{X}_4 - \dot{X}_1\right) - \left(\dot{X}_{cw,out} - \dot{X}_{cw,in}\right). \tag{9}$$

Additionally, to evaluate the performance of the cycle as a whole, the total destroyed exergy is calculated as the sum of each component's destroyed exergy, i.e., $\dot{I}_{tot} = \sum_i \dot{I}_i$.

Ultimately, several indicators were used to compare and establish which working fluid was the most convenient. These are, as suggested in [39]: Thermal Carnot efficiency, Thermal efficiency, Exergetic efficiency, Exergy destruction factor, Volumetric flow ratio and the Size parameter of the turbine. The thermal Carnot efficiency, refers to the maximum theoretical efficiency achievable when a heat engine is placed between two temperatures, and can be evaluated as,

$$\eta_{th,carnot} = 1 - \frac{T_1}{T_3}, \tag{10}$$

where T_1 and T_3 refer to the absolute temperatures at the pump and expander inlet respectively. Meanwhile, the thermal efficiency, is calculated as the ratio between the actual net work $\dot{W}_{net}$ delivered by the cycle and the heat that is supplied to it $\dot{Q}_{in}$, as

$$\eta_{th} = \frac{\dot{W}_{net}}{\dot{Q}_{in}}. \tag{11}$$

The exergetic efficiency relates the net work $\dot{W}_{net}$ with the total input of exergy supplied to it, expressed as follows,

$$\eta_{exg,ORC} = \frac{\dot{W}_{net}}{\dot{X}_{hs,in} - \dot{X}_{hs,out}}. \tag{12}$$

On the other hand, the exergy destruction factor, *EDF*, is a parameter that associates the total exergy destroyed by the cycle to the net work.

$$EDF = \frac{\dot{I}_{tot,ORC}}{\dot{W}_{net}}. \tag{13}$$

In this sense, the higher the *EDF*, the less efficient the ORC will be. To account for the size of the volumetric expansion of the working fluid through the expander, the volumetric flow ratio, *VFR* is evaluated, in the following form,

$$VFR = \frac{\dot{V}_4}{\dot{V}_3}. \tag{14}$$

This value is related to the nature of the working fluid and usually favours refrigerants over alkanes since a lower *VFR* implies a smaller expander. Finally, the size parameter of the turbine, *SP*, offers a first approach of the actual size of the expander [43], where larger values of *SP* indicate higher costs; the parameter *SP* is evaluated as follows,

$$SP = \frac{\sqrt{\dot{V}_4}}{(h_3 - h_{4s})^{1/4}}. \tag{15}$$

2.2. Drying unit for limestone

As shown in Fig. 3, a drying unit constitutes an alternative to recover the available heat from the combustion gases. Instead of an evaporator, a simpler air-cooled heat exchanger is proposed where a fresh air inlet at ambient temperature and moisture, 2% H_2O, reaches T = 170 °C (i.e., an approach of 10 °C) and then enters a direct contact rotary dryer with a wet raw material stream composed of limestone with a particle size distribution of typically 50–75 mm at 16% H_2O content. To avoid condensation inside the equipment, the water content is removed until the exhausted flow is 10 °C above the dew point. The energy and exergy balance equations used for each component of the drying unit are presented below [44].

The heat exchanger unit employs fresh air to cool down the hot gas flow. The heat entering the system, $\dot{Q}_{in}$, is used to produce the dry air required to remove moisture from the solid stream,

$$\dot{Q}_{in} = \dot{m}_{air}(h_{dry} - h_{fresh}), \tag{16}$$

where the air mass flow rate, $\dot{m}_{air}$, is evaluated as follows,

$$\dot{m}_{air} = \dot{m}_{hs}(h_{hs,in} - h_{hs,out})/(h_{dry} - h_{fresh}). \tag{17}$$

The destroyed exergy for the heat exchanger can be expressed as follows,

$$\dot{I}_{HX} = \left(\dot{X}_{hs,in} - \dot{X}_{hs,out}\right) - \left(\dot{X}_{dry} - \dot{X}_{fresh}\right). \tag{18}$$

The rate of evaporated water, $\dot{m}_{ew}$, at the dryer depends on the dry air and solid mass flows and the initial moisture content, related as follows,

$$\dot{m}_{ew} = \frac{\left[\dot{m}_{air}(h_{dry} - h_{exh}) + \dot{m}_{raw,in}(h_{raw,in} - h_{raw,out})\right]}{(h_{exh} - h_{raw,out})}. \tag{19}$$

with the destroyed exergy for this unit defined as,

$$\dot{I}_{dryer} = \left(\dot{X}_{dry} - \dot{X}_{exh}\right) - \left(\dot{X}_{r.aw,out} - \dot{X}_{raw,in}\right). \tag{20}$$

Eqs. (16) to (20) must be solved iteratively once the desired exhaust condition related to the dew point of the current is defined. Finally, the exergy efficiency of the dryer, $\eta_{exg,dryer}$, is estimated as:

$$\eta_{exg,dryer} = 1 - \frac{\dot{I}_{tot,dryer}}{\dot{X}_{hs,in} - \dot{X}_{hs,out}}. \tag{21}$$

2.3. Exergo-economic analysis cost models

An exergo-economic analysis is performed to fully compare the alternatives considered for waste heat recovery at the cement plant described in subsection 1.1. The traditional methodology for exergo-economic studies considers the interactions between the exergy and the average unit costs of the streams [26]. It has been successfully applied for similar analysis i.e. in [15,17,33–35] and it is within the scope proposed for this work.

The general costs balance equation for a system that receives heat and produces work is stated as:

$$\sum \dot{C}_e + \dot{C}_w = \sum \dot{C}_i + \dot{C}_q + \dot{Z}_t, \tag{22}$$

where $\dot{C}_e$, $\dot{C}_w$, $\dot{C}_i$, $\dot{C}_q$ and $\dot{Z}_t$ are respectively the cost rates of the exiting streams, work, entering streams, heat and the sum of the capital investment costs and the operation and maintenance costs rates. Cost rates could also be expressed as the product between the average unit cost and the exergy rate of a stream, as follows,

$$\dot{C}_i = c_i \dot{X}_i, \tag{23}$$

$$\dot{C}_e = c_e \dot{X}_e, \tag{24}$$

$$\dot{C}_w = c_w \dot{W}, \tag{25}$$

$$\dot{C}_q = c_q \dot{X}_q, \tag{26}$$

$$\dot{Z}_t = \dot{Z}^{CI} + \dot{Z}^{OM}. \tag{27}$$

The total capital cost of the investment, Z^{CI}_{tot}, and maintenance, $\dot{Z}^{OM}$ are easily obtainable from the APEA software. However, to calculate the capital investment costs rate, $\dot{Z}^{CI}$ it is necessary to annualise the total capital costs using the capital recovery factor, *CRF*,

$$CRF = \frac{A}{P} = \frac{i_{eff}(1 + i_{eff})^n}{(1 + i_{eff})^n - 1}, \tag{28}$$

which in turn depends on the effective rate of return i_{eff}. Such rate is calculated in terms of the nominal rate of return as,

$$i_{eff} = \left(1 + \frac{i}{n}\right)^n - 1. \tag{29}$$

The *CRF* is the ratio used to calculate the present value of an annuity of equal payments, where *A*, the annualised value, equals the aforementioned capital investment costs rate $\dot{Z}^{CI}$, being *P*, the present value; that is, the total capital costs of the investment.

The variable *n* in Eqs. (28) to (29) is the number of periods (years) for the cash-flow and it coincides with the project financial life. From now on, it is set at 20 years. Also, as recommended in [45] for a medium level of investment risk, a 20% nominal rate of return, *i*, should be used in the preliminary analyses.

All process equipment was selected based on recommendations reported in the literature [46]. In regard to the ORC, shell and tube heat exchangers were used in the evaporator, as well as a centrifugal pump and a non-condensing turbine. For the drying unit, a shell and tube heat exchanger and a direct contact rotary dryer were included. Likewise, they were mapped and sized using the software and the costs brought to the present, i.e. 2020. A centrifugal fan is required to blow the fresh air through the drying unit and it is modelled as an isentropic compressor with a pressure increase of 6.9 kPa and all the associated electricity costs were added to the operation and maintenance costs of the entire unit. However, the capital costs of the said fan are neglected as there are similar existing units available in the plant.

The unit price of the cooling water, the purchased electricity from the grid and the fuel are c_{cw}=0.027 \$/m^3 [42], c_{el}=0.07 \$/kWh [42] and c_{fuel}=3.84 \$/GJ [15], respectively. The latter was obtained for a cement plant and it comprises the cost of the entering exergy of several fuel sources.

Finally, by combining Eqs. (22) to (27) it is possible to calculate the unit costs of power generation and the dry solid flow. For a fixed rate of return:

$$c_w = \dot{Z}_t / \dot{W}_{net}, \tag{30}$$

and

$$c_{raw,out} = \dot{Z}_t / \dot{X}_{raw,out}. \tag{31}$$

Eq. (30) is useful to compare the economic performance of the ORC arrangements. The lower the unit cost of power generation, the better. This parameter has the same meaning as the specific cost of electricity generation that has been widely reported in the literature to allow the economic optimisation of the cycle as in [19,23,24,31]. Other economic parameters to be considered are the cost of the destroyed exergy valued as fuel, $\dot{C}_D$, (see Eq. (32)), and the exergo-economic factor, f_k, (defined in Eq. (32)). The first refers to the potential economic loss of not taking advantage of the invested resources, and is defined as follows,

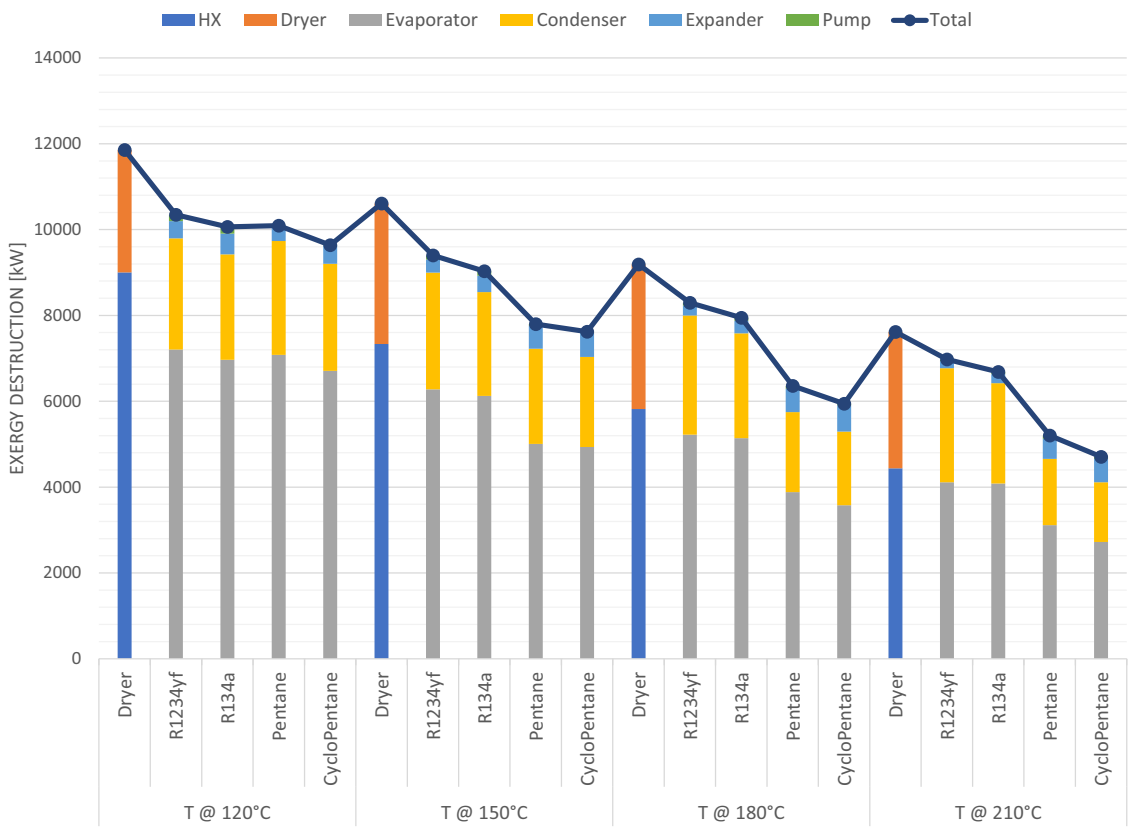

Fig. 4. Total exergy destruction and by component.

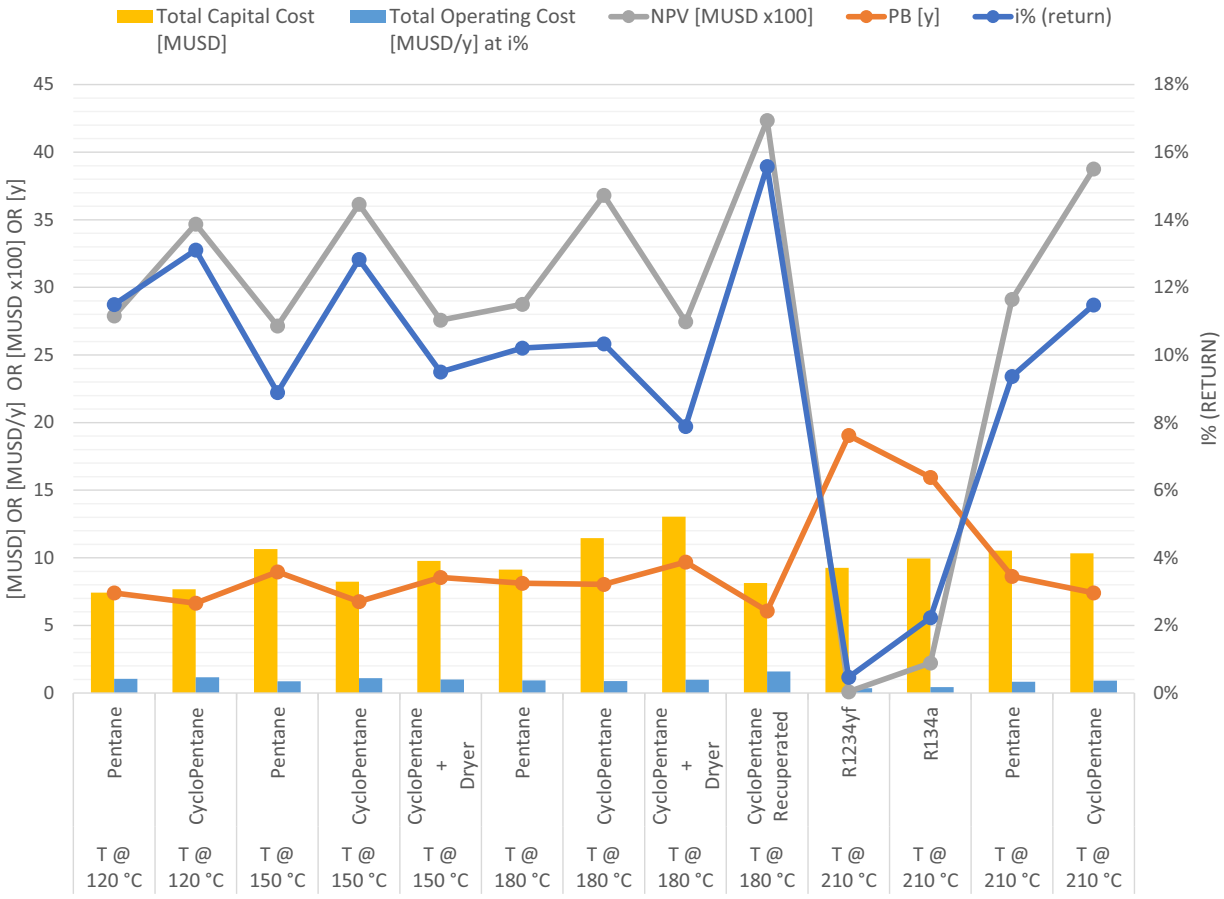

Fig. 5. Economic indicator for the alternative with positive *NPV*.

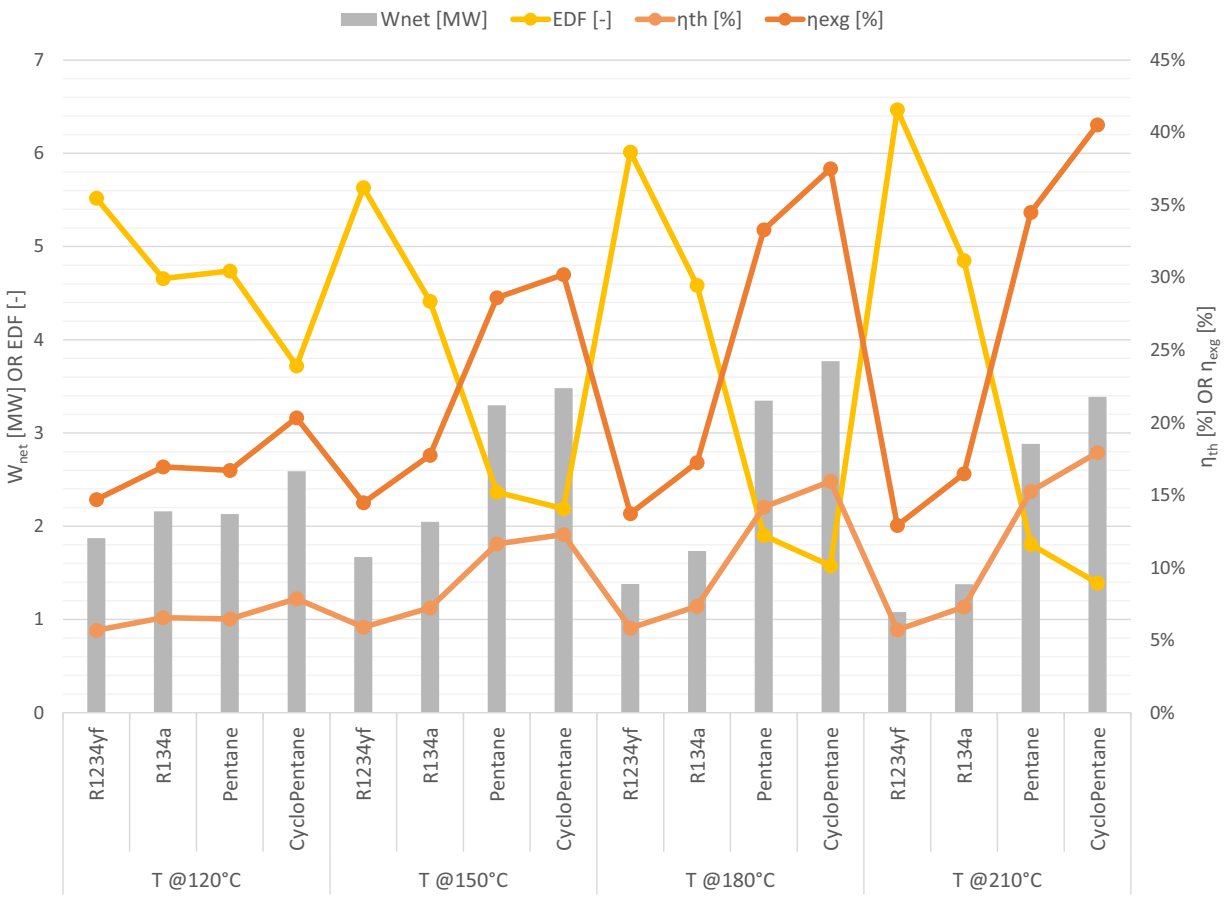

Fig. 6. Thermal, exergetic efficiencies and net work for the ORCs.

$$\dot{C}_D = c_{fuel}\dot{I}_{tot}. \tag{32}$$

On the other hand, the exergo-economic factor, relates the capital and operating costs of each alternative to the cost of the exergy destroyed by it, in the subsequent manner,

$$f_k = \frac{\dot{Z}_t}{\dot{Z}_t + \dot{C}_D}. \tag{33}$$

It follows that a low value of f_k suggests that cost savings might be achieved by improving efficiency (i.e., reducing the exergy destruction), even if the capital investment costs increase. On the other hand, a high value of the factor suggests a decrease in the investment costs at the expense of its exergetic efficiency [26].

Despite how useful these parameters (C_D and f_k) are, they work on a fixed rate of return that throws unit costs far from those of market conditions. To better compare and choose between the power cycle and the drying unit a "sale price" for electricity and for the exergy that accompanies the dry solids must be defined as equal to the purchase prices indicated above. The drying unit acts as a feed pre-heater for the kiln, therefore, it is a valid assumption to value such exergy (i.e., the one entering with the dry solids), like fuel savings. Eventually, Eq. (30) must be equal to Eq. (34). The simple system of equations that appears must be solved varying the return rate embedded in $\dot{Z}_t$.

$$\dot{C}^*_w = c_{el}\dot{W}_{net}, \tag{34}$$

$\dot{C}^*_w$ being the cost rate of selling the generated power at market conditions.

The parameters used to compare the investments are the net present value, (*NPV*), and the payback time (PB). The first one relates the annualised cash-flow, R_t, and the rate of return i, as follows,

$$NPV = \sum_{z=0}^{n} \frac{R_t}{(1+i)^z}, \tag{35}$$

where z is the period, and n is the total number of periods. The payback time (PB) is defined as,

$$PB = \frac{\dot{Z}^{CI}_{tot}}{R_t}. \tag{36}$$

As expected, a negative *NPV* indicates that the cash-flow of the investment is not economically viable; higher values of *NPV* and i are preferred while a lower *PB* value is desirable.

3. Results and discussion

The methodology defined in the previous sections allows each of the heat recovery alternatives to be addressed from the point of view of energy, exergy, and costs. In turn, various performance parameters were defined. Although the base case to be evaluated is when hot gases leave the pre-conditioning tower at T = 180 °C, this single design point does not grant a holistic view of the heat recovery potential in the cement plant. For this reason, a brief sensitivity analysis was carried out, varying the outlet temperature of those gases. There is a compendium of the most important parameters for the drying unit and the ORCs at outlet temperatures of T = 120 °C , T = 150 °C, T = 180 °C and T = 210 °C in Table A.1, A2, A3 and A4, respectively. Likewise, Fig. 4 summarises the information associated with

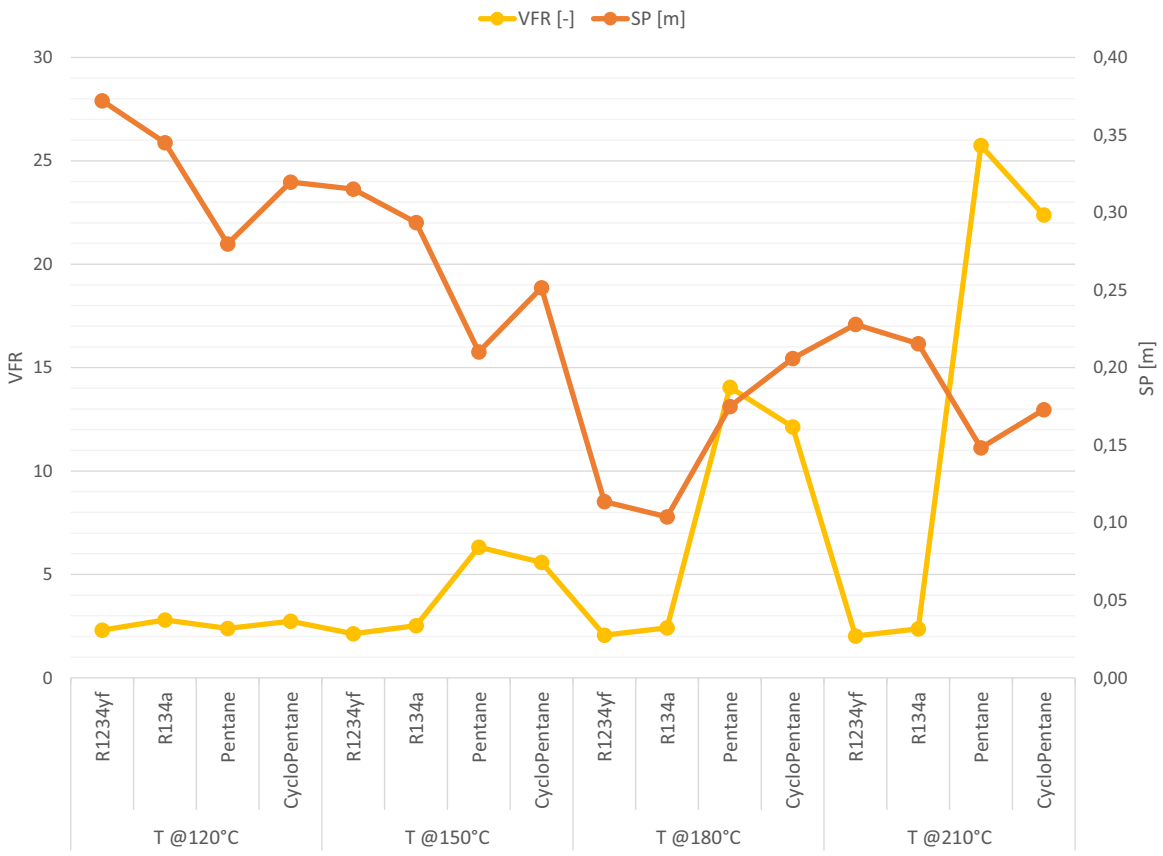

Fig. 7. VFR and SP [m] parameters for the ORCs.

the total destruction of exergy and by components and Fig. 5 displays the main cost indicators for the alternatives with positive *NPV*. It is simpler and more convenient first to analyse separately the ORCs and the drying units and then reach to a consensus on an economic basis.

3.1. ORCs:

In general, higher temperatures imply greater thermal and exergetic efficiency of the cycles, as well as lesser total exergy destruction. Fig. 4 clearly shows this trend, while quickly identifying the working fluid that best behaves according to this criterion; for any of the evaluated cases it is Cyclo-Pentane. Fig. 4 also shows the distribution of the exergy destruction by each individual component of the cycle. Based on the averages of all cases, the greatest destroyer of exergy is the evaporator, 64.3%, followed by the condenser, 29.2%, the expander, 5.6%, and the pump with 0.85% of the total. The averaged values are somewhat biased due to the influence of temperature and the nature of the fluids, that is, alkanes destroy larger quantities of exergy than the refrigerants in the expander. This is notable at higher temperatures when it is around 10% of the total, undoubtedly, far from the average.

It can be seen from Fig. 6 that the highest exergetic efficiency of 40.54% is achieved when the ORC operates with Cyclo-Pentane at an outlet temperature of the hot gases of $T = 210\ ^{\circ}C$. However, efficiency alone does not inform performance in terms of the work delivered by the cycle. The highest net work is found at $T = 180\ ^{\circ}C$, which is the base case, and it is 3.77 MW. With these results, one would be inclined to think that with lower temperatures, the generated work would be greater due to the larger heat entry to the cycle. This reasoning, however, is tendentious. Although the amount of energy received by the cycle is important, its quality decreases with temperature. Therefore, it translates into the existence of an optimal operating point that is different if the goal is to maximise net work produced or the efficiency.

A performance parameter that partially settles this discussion is the *EDF*, since it relates the total destroyed exergy to the net work. The lower its value, the better the performance of the system. That said, in the evaluated cases, the *EDF* trend (shown in Fig. 6) is somewhat inverse to the exergetic efficiency of the cycle. The lower values are found when the exergetic efficiency peaks, that is, when the working fluid is Cyclo-Pentane. The lowest value, *EDF* = 1.39, coincides with $T = 210\ ^{\circ}C$.

The *VFR* and *SP* parameters, which account for the volumetric expansion of the working fluid and the actual size of the expander, are higher for the alkanes than for the refrigerants as seen in Fig. 7. High values of *VFR* signify a lower attainable efficiency in the turbine, while large values of *SP* indicate an increment in the capital costs of the expander and in turn can be also a limiting disadvantage when space availability is a constraint. In both cases, a lower value is desirable. Thus, the working fluid with the best performance in such circumstances is R1234yf. The smallest value of *VFR*, *VFR* = 2.02, is obtained when the temperature of the heat source is $T = 210\ ^{\circ}C$. Despite this, the lowest *SP* = 0.1 m is achieved in the case when $T = 180\ ^{\circ}C$ with R134a as working fluid, and it is followed closely by an *SP* = 0.11 m for R1234yf at the same temperature. It is said in [47] that expander efficiencies superior to 80% are only reachable for values of $VFR < 50$. Fortunately, values outside this range are not found for any of the cases considered.

3.2. Drying unit:

For this unit to operate correctly, it is necessary to ensure that there is no condensation inside it. This is the reason why the case evaluated for the lowest temperature of the hot gases is at $T = 120\ ^{\circ}C$. The performance of the drying system can be described in two ways. The first way, using the amount of exergy destroyed in the system, indicates that at higher temperatures less exergy is destroyed (see

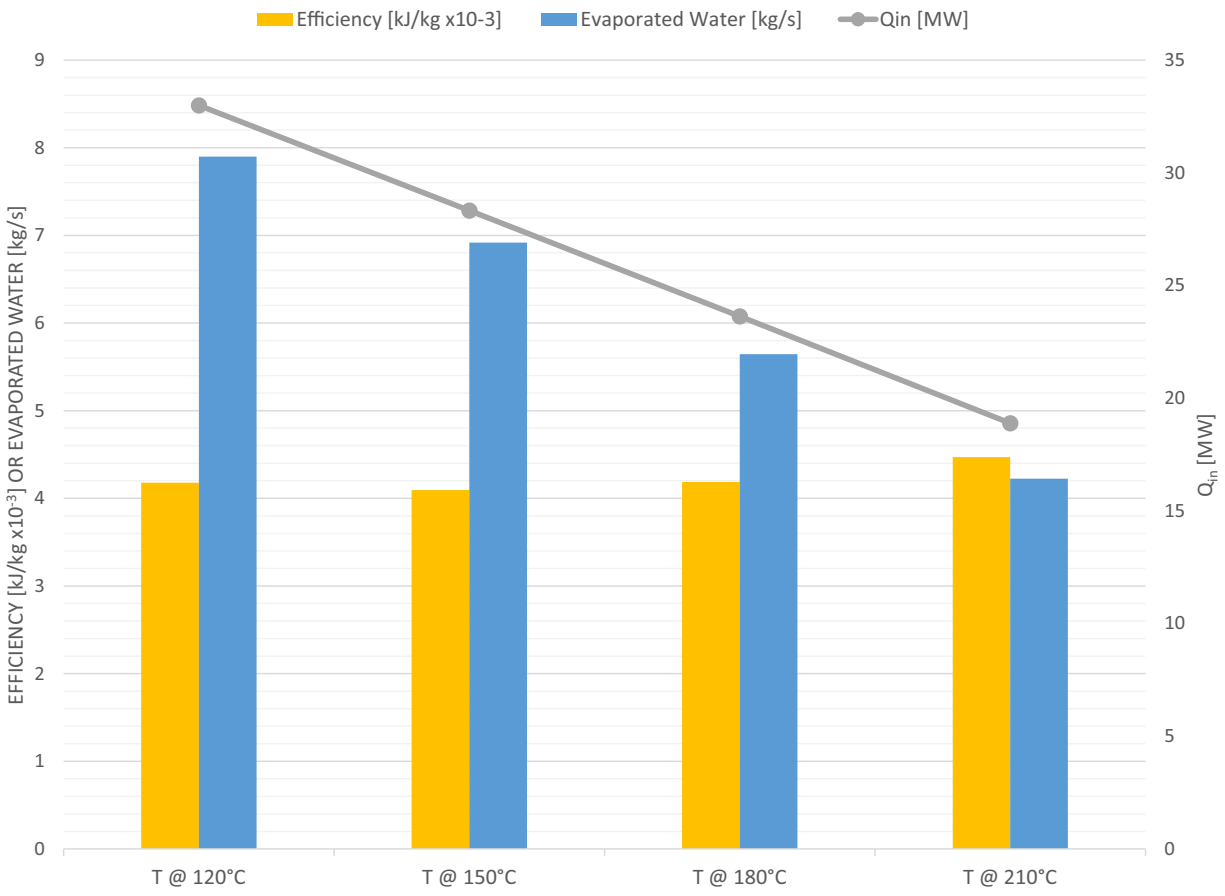

Fig. 8. Heat input and thermal efficiency for the drying unit.

Fig. 4) and that the gas/gas heat exchanger accounts on average for 2/3 of the total. The second, is much more significant, as it accounts for the use of the total heat received to evaporate water. Such a sort of thermal efficiency (defined in [46]) is presented in Fig. 8. It is noticeable that lower temperatures mean less employment of heat per unit of evaporated water. Despite such a trend, there is an optimal value, which can be found to achieve the best efficiency. An optimal value occurs because the dryer performance is coupled with the incoming fresh airflow (shown in Fig. 9) and it is greater at lower temperatures. The best efficiency, η_{th} = 4095.16 kJ/kg, is found when T = 150 °C. The rate of evaporated water depends strongly on the heat input to the system. In this sense, the higher rate, $\dot{m}_{ew}$ = 7.9 kg/s, is obtained at T = 120 °C. Likewise, it is in this case when the minimum final moisture of the solids, 10.33%, occurs.

3.3. Costs:

ORCs are initially compared at a fixed rate of return of 20% as shown in Fig. 11. It is appreciated that the lowest cost of the destroyed exergy is held by Cyclo-Pentane and this result is in agreement with Fig. 4, where the usage of this working fluid destroys the least exergy. Unit costs of power generation are in line with this trend, and the lowest cost, c_w = 0.12 $/kWh, appears at T = 150 °C. The exergo-economic factor is somewhat inverse to this trend and it reaches its highest value, f_k = 0.87, at T = 210 °C. In Fig. 11, it is also observed that the highest costs for both generated (accompanying the dry solids stream) and destroyed exergy are produced by the drying units. These are increased if the temperature of the hot gases decreases. Then, it can be affirmed that the costs of the investment are somewhat concentrated in those associated with exergy. In consequence, it would be ideal to maintain high temperatures to accomplish greater efficiencies in the process.

The design points with the best behaviours of the unit cost and the exergo-economic factor do not coincide. That is why the *NPV* is used. Simply, the option with the highest value, *NPV* = 0.88, is chosen for the ORC that works with Cyclo-Pentane at T = 180 °C. The differences between the indicators lie mainly in the capital and operating costs for each case. In turn, these are influenced by the size and operating conditions of the process equipment. The purely economic indicator (*NPV*) is preferred because it facilitates comparisons.

Now, when the amount of evaporated water is taken into account, its maximum can be achieved at a higher unit cost. Depending on the intention of the process, this can be a relevant variable (i.e., when a drier supply of raw meal is required by the mill).

A fixed-rate of return analysis is far from actual market conditions and could over-predict the economic performance of an investment. To fill this gap Eqs. (30) and (34) are used. The alternatives with positive *NPV* are recorded in Fig. 5. Essentially, when unlimited capital of investment is considered, the highest net present value, *NPV* = 0.38 MUSD, is obtained when the ORC operates at T = 210 °C. However, such a temperature is higher than the allowable one, due to process and material constraints. Therefore, the second alternative, *NPV* = 0.37 MUSD at T = 180 °C with the same working fluid, is the one that should be selected. The payback time for the latter is *PB* = 8.04 years at a rate of return of 10.33%. Remarkably, none of the drying units present a positive *NPV* since the unit cost of the saved fuel in the kiln is much lower than the unit cost of electricity because of the Colombian electricity prices. Regardless, there are some benefits attainable when a drying unit is employed that cannot be directly quantified, like increasing the available grinding capacity by entering drier material to the mill. Then, it is logical to consider the option of placing a

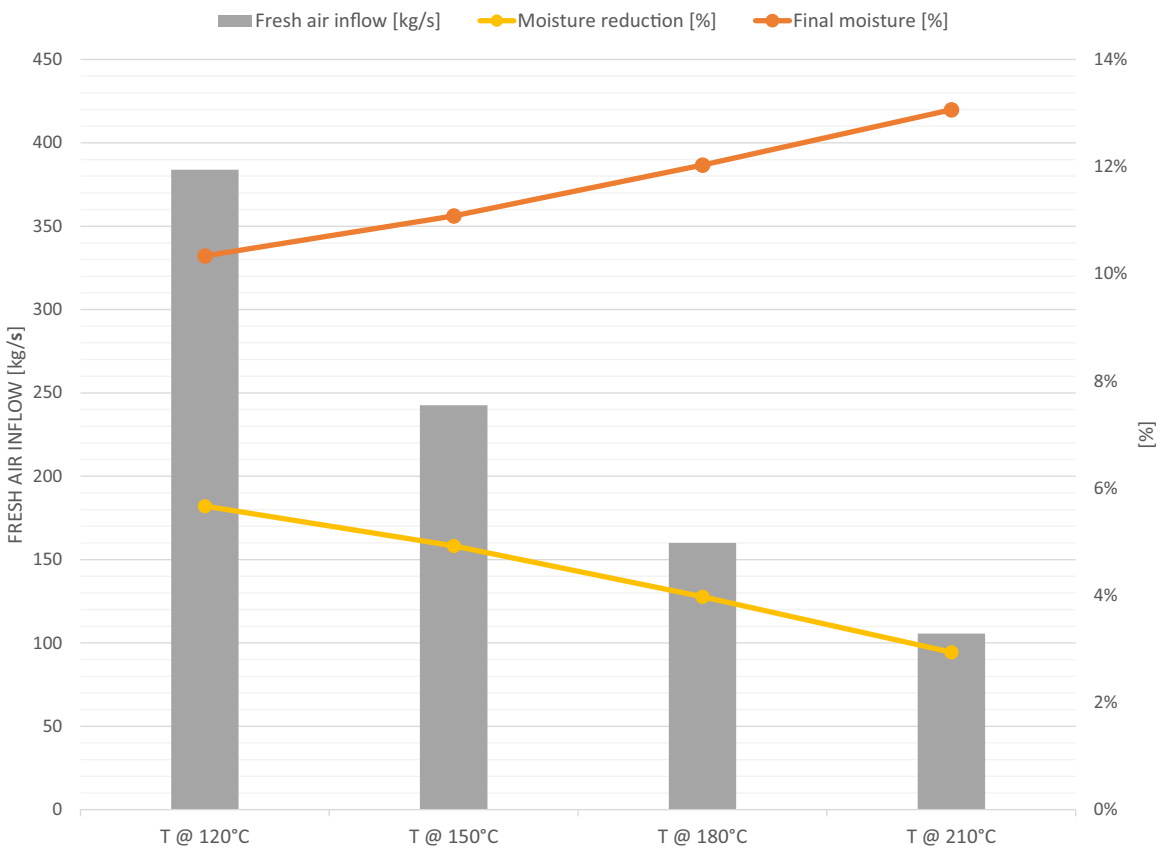

Fig. 9. Fresh air inflow to the dryer and final moisture content of the solids.

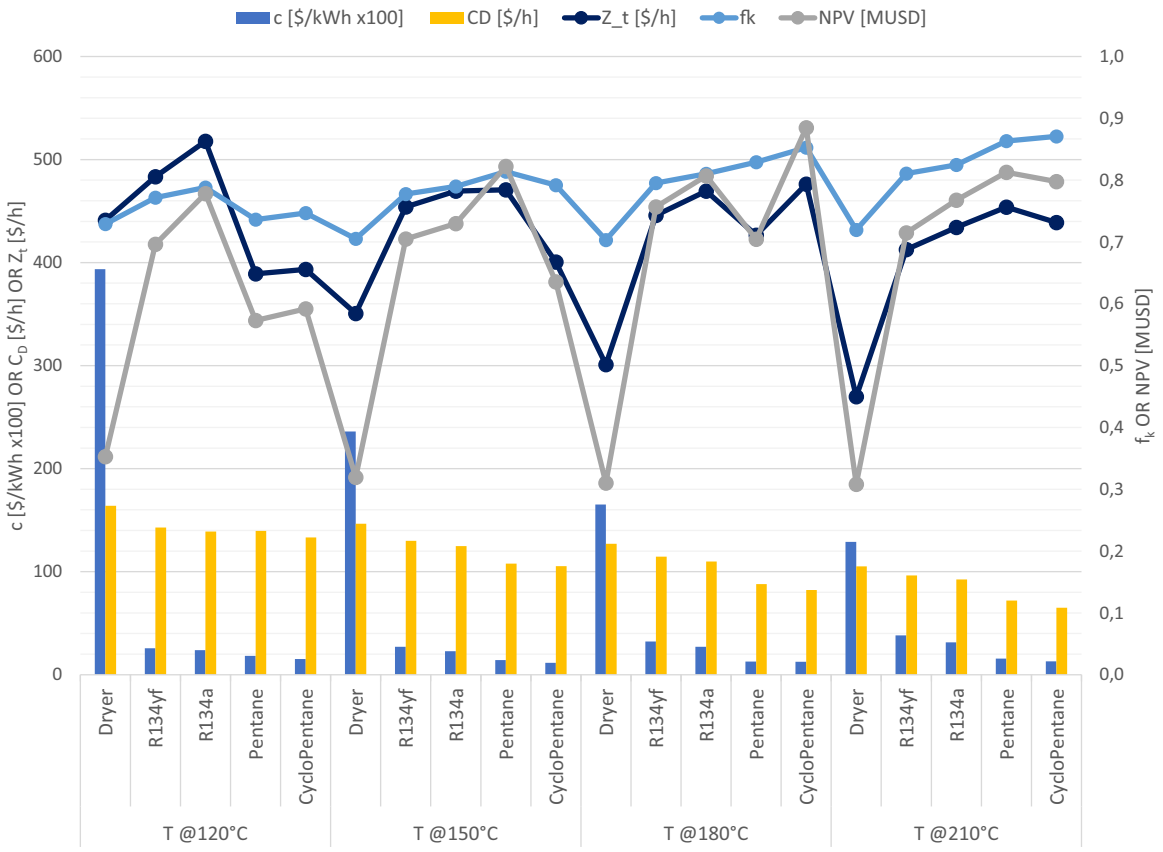

Fig. 11. Exergo-economic factor, cost of destroyed exergy and unit cost of power generation or the dry solids stream at a fixed rate of return of 20%.

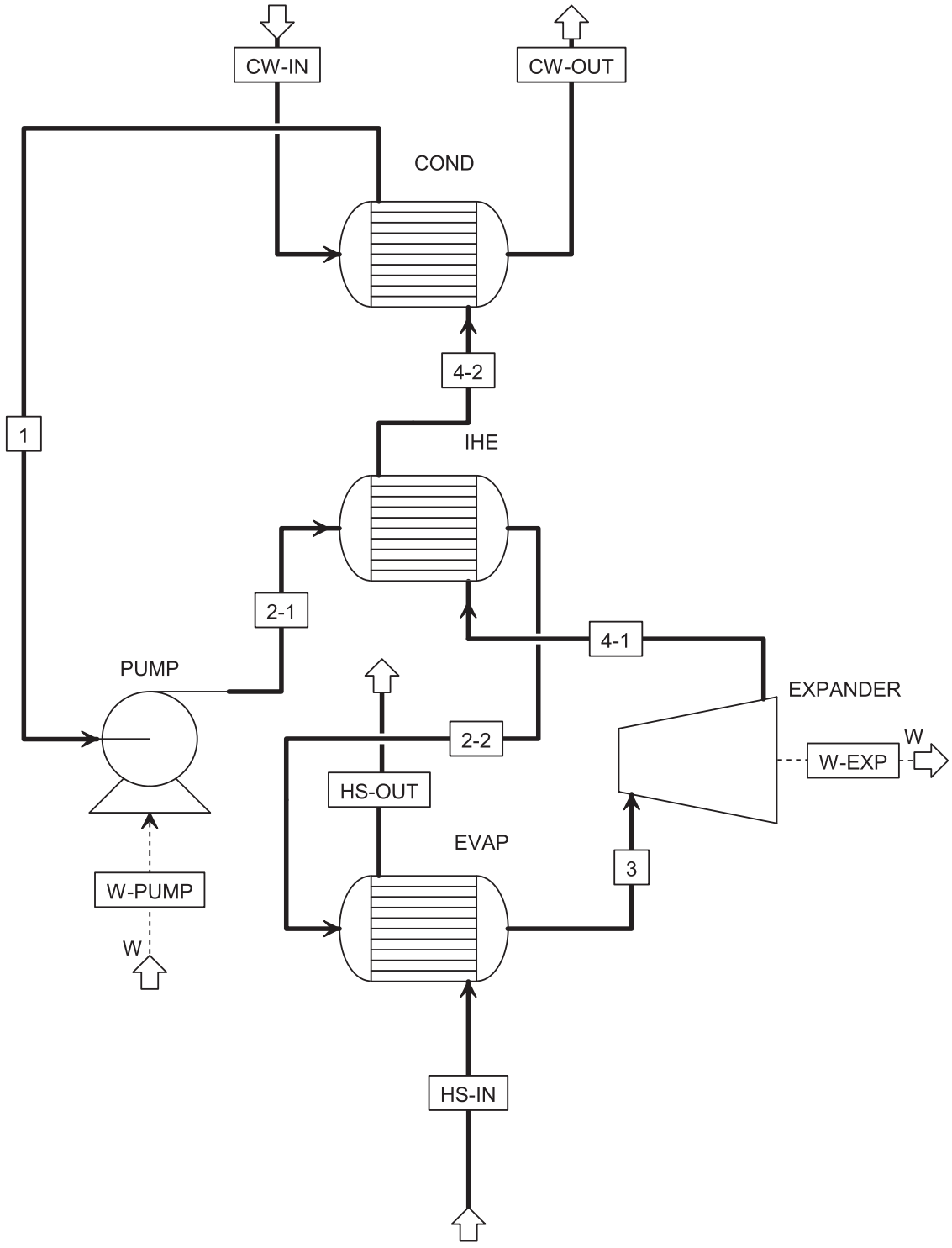

Fig. 10. Recuperated ORC schematics.

dryer that finishes cooling the hot gases to T = 120 °C after the ORCs with the best *NPV* to completely recover all the available heat. Such ORCs operate at T = 150 °C and T = 180 °C with Cyclo-Pentane as working fluid. The parameters of these configurations are reported in Tables A5 ro A6. Calculations showed that exergetic efficiency shyly improves, 1.2% (T = 150 °C), or worsens, 3.5% (T = 180 °C), compared to ORC alone. Thus, when estimating the *NPV* with market prices for fuel and electricity, it is found that despite remaining positive in both cases, *NPV* ∼ 0.27 MUSD (Fig. 5), the investment would be less profitable than simply using an ORC.

Although the simple ORC is sufficient to withstand the screening process to determine the best working fluid and operation conditions through the exergo-economic analysis of a hot effluent, complex variations of such power cycle make sense when better performance is required. In fact, there are various modifications that can be carried out to the organic Rankine Cycle, for example, several stages of preheating in the evaporator or successive expansion can be included. However, to make investment decisions, this additional complexity must be justified in terms of thermodynamic and economic performance. For this reason, it is advisable to go from the simple to the

complex, identifying the configurations with the greatest potential and then gradually increasing the cycle complexity, while verifying that the expected improvement is achieved.

Once the most suitable operating conditions and working fluid have been found in terms of exergy and economic performance for a simple ORC system, it is feasible to improve its performance indicators by transforming the cycle into a recuperated one, that is, to include an internal heat exchanger as shown in Fig. 10. The purpose of the said *IHE* is to preheat the feed to the evaporator, in this way, the average evaporation temperature is increased and the average condensing temperature is reduced [29], simultaneously contributing to the efficiency of the cycle and the reduction of the area required by the evaporator and condenser. The base case is used, with Cyclo-Pentane at T = 180 °C and the evaporator feed temperature at which the maximum work occurs, T = 82 °C. It is found that such recuperated ORC could deliver 4.1 MW of electricity with an *NPV* = 0.42 MUSD, a rate of return of 15.58% and a payback time of *PB* = 6.07 years. This is 8.75% more work with 13.51% better economic performance than the simple ORC. Such notable improvement is easily explained as the combination of two favourable and interdependent situations, the delivered net work increases, improving the energy and exergy efficiency of the cycle, and the reduction of the total capital cost, as shown in Fig. 5. The latter is justified with the decrease of the total required area of heat exchange despite the inclusion of extra equipment. The improvements achieved with this configuration are seen in all the performance indicators and can be verified in Table A3. Changes and optimisations like this one could be done to find the best possible answer to the problem of waste heat recovery, however, such a process is beyond the scope of this work and should be considered for the future.

4. Conclusions

In this work, it was evaluated the recovery of waste heat from a hot gas effluent through a sensitivity analysis in which various outlet temperatures were analysed for generating electricity or drying the wet raw material stream of limestone entering the cement production process as feed stock. Different working fluids were examined in the case of ORCs and it was found that alkanes perform better than refrigerants when it comes to high temperatures.

The best alternative is selected based on the *NPV*, calculated for a sale price of electricity of c_{el}=0.07 $/kWh [42]. It is an ORC that operates at T = 180 °C with Cyclo-Pentane as the working fluid with a net present value of *NPV* = 0.37 MUSD, a rate of return of 10.33% and a payback time of *PB* = 8.04 years. Such a power cycle delivers 3.77 MW of net work with a thermal efficiency of η_{th}=15.96% and an exergetic efficiency of η_{exg}=37.52% as shown in Fig. 6 and it meets the constraint that filter materials must not exceed T = 180 °C.

Although having lower capital and operating costs than ORCs as shown in Fig. 11, except at T = 120 °C, none of the drying units has a positive *NPV*. This is explained as a consequence of the lower unit cost of sale of the exergy that accompanies the dry solids stream, c_{fuel}=3.84 $/GJ [15], when compared to electricity. This analysis did not consider economically all the benefits that the use of a dryer can bring, for example, the expansion of the available grinding capacity of the raw material mill. If this parameter becomes relevant to maintain the integrity of the production process, it should be borne in mind that better performance, stated as heat supplied to the amount of evaporated water, is obtained when lower temperatures are used in the gases, which also means, larger fresh air inflows. The maximum moisture reduction is reached when T = 120 °C and it is 5.67% for solids that enter at 16% water content, as shown in Fig. 9. The option of placing a drying unit immediately after an ORC to completely cool down the gases was economically analysed for ORC cases with best *NPV*, T = 150 °C and T = 180 °C. But no substantial improvement was found over using the ORC alone.

Finally, the possibility to improve the simple ORC performance is explored through the inclusion of an internal heat exchanger, as shown in Fig. 10. The recuperated cycle outperforms its simpler configuration in terms of thermal and economic performance delivering 4.1 MW of net work with an *NPV* = 0.42 MUSD, a rate of return of 15.58% and a payback time of *PB* = 6.07 years. This is 8.75% more work with 13.51% better economic performance than the simple ORC.

Certainly, the present work does not correspond to an economic optimisation. However, it presents an adequate approximation of the relevant heat recovery alternatives for the selected effluent, combustion gases at a high temperature, T = 350 °C. In future work, it would be interesting to increase the level of detail of the equipment involved and build a more accurate cost framework limited to the operating conditions that present a better performance in economic terms.

Declaration of Competing Interest

The authors declare that they have no known competing financial interests or personal relationships that could have appeared to influence the work reported in this paper.

Acknowledgements

This research is funded by the The Royal Academy of Engineering through the Newton-Caldas Fund IAPP18-19\218 project that provides a framework where industry and academic institutions from Colombia and the UK collaborate in heat recovery in large industrial systems.

Appendix. A

Table A1
Performance indicators for each alternative @120 °C exhaust.

T @120°C	Dryer	R1234yf	R134a	Pentane	Cyclo-Pentane
η_{carnot} [%]	-	13.05%	13.05%	13.05%	13.05%
η_{th} [%]	4177.09*	5.68%	6.55%	6.46%	7.85%
η_{exg} [%]	6.96%	14.70%	16.95%	16.71%	20.33%
I_{tot} [kW]	11857.31	10343.59	10061.93	10091.92	9638.91
EDF [-]	-	5.52	4.66	4.74	3.72
VFR [-]	-	2.31	2.80	2.39	2.74
SP [m]	-	0.37	0.35	0.28	0.32
P_{evap} [bar]	-	33	40	5	4
T_{evap} [°C]	-	110	110	110	110
P_{cond} [bar]	-	16.46	16.88	2.13	1.43
Q_{in} [kW]	32990.08	32990.08	32990.08	32990.08	32990.08
W_{pump} [kW]	-	593.80	669.07	53.93	38.32
$W_{turbine}$ [kW]	-	2467.55	2829.40	2183.63	2628.93
W_{net} [kW]	-	1873.75	2160.33	2129.70	2590.61

*kJ supplied/kg evaporated water

Table A2
Performance indicators for each alternative @150 °C exhaust.

T @150°C	Dryer	R1234yf	R134a	Pentane	Cyclo-Pentane
η_{carnot} [%]	-	19.36%	19.36%	19.36%	19.36%
η_{th} [%]	4095.16*	5.89%	7.22%	11.64%	12.29%
η_{exg} [%]	7.92%	14.49%	17.76%	28.62%	30.22%
I_{tot} [kW]	10608.98	9400.61	9030.29	7800.27	7619.57
EDF [-]	-	5.63	4.41	2.37	2.19
VFR [-]	-	2.14	2.52	6.32	5.58
SP [m]	-	0.32	0.29	0.21	0.25
P_{evap} [bar]	-	33	40	12	8
T_{evap} [°C]	-	140	140	140	140
P_{cond} [bar]	-	16.46	16.88	2.13	1.43
Q_{in} [kW]	28328.52	28328.52	28328.52	28328.52	28328.52
W_{pump} [kW]	-	393.15	442.80	145.05	77.02
$W_{turbine}$ [kW]	-	2062.41	2488.84	3442.50	3558.30
W_{net} [kW]	-	1669.26	2046.04	3297.45	3481.29

*kJ supplied/kg evaporated water

Table A3
Performance indicators for each alternative @180 °C exhaust.

T @180°C	Dryer	R1234yf	R134a	Pentane	Cyclo-Pentane	Cyclo-Pentane Recuperated
η_{carnot} [%]	-	24.82%	24.82%	24.82%	24.82%	24.82%
η_{th} [%]	4186.20*	5.84%	7.33%	14.17%	15.96%	17.35%
η_{exg} [%]	8.57%	13.72%	17.24%	33.30%	37.52%	40.80%
I_{tot} [kW]	9189.86	8294.54	7947.02	6360.35	5944.08	5619.90
EDF [-]	-	6.01	4.59	1.90	1.58	1.37
VFR [-]	-	2.06	2.42	14.05	12.13	12.13
SP [m]	-	0.11	0.10	0.17	0.21	0.21
P_{evap} [bar]	-	33	40	22	16	16
T_{evap} [°C]	-	170	170	170	170	170
P_{cond} [bar]	-	16.46	16.88	2.13	1.43	1.43
Q_{in} [kW]	23627.87	23627.87	23627.87	23627.87	23627.87	23627.87
W_{pump} [kW]	-	270.94	309.23	228.05	133.11	144.75
$W_{turbine}$ [kW]	-	1650.17	2042.04	3575.17	3903.73	4245.21
W_{net} [kW]	-	1379.22	1732.80	3347.12	3770.62	4100.46

*kJ supplied/kg evaporated water

Table A4
Performance indicators for each alternative @210 °C exhaust.

T @210°C	Dryer	R1234yf	R134a	Pentane	Cyclo-Pentane
η_{carnot} [%]	-	29.59%	29.59%	29.59%	29.59%
η_{th} [%]	4471.04*	5.71%	7.29%	15.26%	17.94%
η_{exg} [%]	8.90%	12.91%	16.48%	34.49%	40.54%
I_{tot} [kW]	7614.40	6977.88	6684.10	5204.65	4707.64
EDF [-]	-	6.47	4.85	1.81	1.39
VFR [-]	-	2.02	2.37	25.74	22.38
SP [m]	-	0.23	0.22	0.15	0.17
P_{evap} [bar]	-	33	40	33	26
T_{evap} [°C]	-	200	200	200	200
P_{cond} [bar]	-	16.46	16.88	2.13	1.43
Q_{in} [kW]	18887.17	18887.17	18887.17	18887.17	18887.17
W_{pump} [kW]	-	184.86	213.52	267.40	169.19
$W_{turbine}$ [kW]	-	1263.74	1591.31	3150.43	3557.87
W_{net} [kW]	-	1078.88	1377.78	2883.03	3388.69

*kJ supplied/kg evaporated water

Table A5
Performance indicators for the combined ORC+Dryer system @150 °C exhaust.

T @150°C	Cyclo-Pentane	Dryer	ORC+Dryer
η_{carnot} [%]	19.36%	-	-
η_{th} [%]	12.29%	12221.60*	-
η_{exg} [%]	30.22%	8.1%	31.40%
I_{tot} [kW]	7619.57	1123.39	8742.96
EDF [-]	2.19	-	-
VFR [-]	5.58	-	-
SP [m]	0.25	-	-
P_{evap} [bar]	8.00	-	-
T_{evap} [°C]	140.00	-	-
P_{cond} [bar]	1.43	-	-
Q_{in} [kW]	28328.52	4661.52	32990.05
W_{pump} [kW]	77.02	-	-
$W_{turbine}$ [kW]	3558.30	-	-
W_{net} [kW]	3481.29	67.87	-

*kJ supplied/kg evaporated water

Table A6
Performance indicators for the combined ORC+Dryer system @180 °C exhaust.

T @180°C	Cyclo-Pentane	Dryer	ORC+Dryer
η_{carnot} [%]	24.82%	-	-
η_{th} [%]	15.96%	6370.50*	-
η_{exg} [%]	37.52%	8.4%	34.01%
I_{tot} [kW]	5944.08	2466.31	8410.39
EDF [-]	1.58	-	-
VFR [-]	12.13	-	-
SP [m]	0.21	-	-
P_{evap} [bar]	16.00	-	-
T_{evap} [°C]	170.00	-	-
P_{cond} [bar]	1.43	-	-
Q_{in} [kW]	23627.87	9362.21	32990.08
W_{pump} [kW]	133.11	-	-
$W_{turbine}$ [kW]	3903.73	-	-
W_{net} [kW]	3770.62	99.12	-

*kJ supplied/kg evaporated water

References

[1] A.K. Chatterjee, Cement Production Technology, 66, CRC Press, 2018, doi: 10.1201/9780203703335.

[2] L. Lopera, C. Nieto, A.C. Escudero, C.A. Bustamante, M.C. Fernández, Evaluation of low-temperature waste heat recovery technologies for the cement industry, WIT Trans. Ecol. Environ. 195 (2015) 111–122, doi: 10.2495/ESUS150101.

[3] W.B.C.f. S. Development, The cement sustainability initiative 66 (2012) 37–39.

[4] T. Gerres, J.P. Chaves Ávila, P.L. Llamas, T.G. San Román, A review of cross-sector decarbonisation potentials in the european energy intensive industry, J. Clean. Prod. 210 (2019) 585–601, doi: 10.1016/j.jclepro.2018.11.036.

[5] C. Bataille, M. Åhman, K. Neuhoff, L.J. Nilsson, M. Fischedick, S. Lechtenböhmer, B. Solano-Rodriquez, A. Denis-Ryan, S. Stiebert, H. Waisman, O. Sartor, S. Rahbar, A review of technology and policy deep decarbonization pathway options for making energy-intensive industry production consistent with the paris agreement, J. Clean. Prod. 187 (2018) 960–973, doi: 10.1016/j.jclepro.2018.03.107.

[6] B. Egilegor, H. Jouhara, J. Zuazua, F. Al-Mansour, K. Plesnik, L. Montorsi, L. Manzini, ETEKINA: Analysis of the potential for waste heat recovery in three sectors: aluminium low pressure die casting, steel sector and ceramic tiles manufacturing sector, Int. J. Thermofluids 1–2 (2020) 100002, doi: 10.1016/j.ijft.2019.100002.

[7] D. Brough, H. Jouhara, The aluminium industry: a review on state-of-the-art technologies, environmental impacts and possibilities for waste heat recovery, Int. J. Thermofluids 1–2 (2020) 100007, doi: 10.1016/j.ijft.2019.100007.

[8] I.F.C. Institute for Industrial Productivity, Waste Heat Recovery for the Cement Sector: Market and Supplier Analysis (June) (2014) 81.

[9] C. Forman, I.K. Muritala, R. Pardemann, B. Meyer, Estimating the global waste heat potential, Renew. Sustain. Energy Rev. 57 (2016) 1568–1579, doi: 10.1016/j.rser.2015.12.192.

[10] G.P. Panayiotou, G. Bianchi, G. Georgiou, L. Aresti, M. Argyrou, R. Agathokleous, K.M. Tsamos, S.A. Tassou, G. Florides, S. Kalogirou, P. Christodoulides, Preliminary assessment of waste heat potential in major European industries, Energy Procedia, 123, Elsevier Ltd, 2017, pp. 335–345, doi: 10.1016/j.egypro.2017.07.263.

[11] H. Jouhara, N. Khordehgah, S. Almahmoud, B. Delpech, A. Chauhan, S.A. Tassou, Waste heat recovery technologies and applications, Therm. Sci. Eng. Progress (2018), doi: 10.1016/j.tsep.2018.04.017.
[12] A. Atmaca, R. Yumrutaş, Thermodynamic and exergoeconomic analysis of a cement plant: part i methodology, Energy Convers. Manag. 79 (2014) 790–798, doi: 10.1016/j.enconman.2013.11.053.
[13] N.A. Madlool, R. Saidur, M.S. Hossain, N.A. Rahim, A critical review on energy use and savings in the cement industries, Renew. Sustain. Energy Rev. 15 (4) (2011) 2042–2060, doi: 10.1016/j.rser.2011.01.005.
[14] International Energy Agency (IEA), World energy outlook | 2016, OECD, 2016, doi: 10.1787/weo-2016-en.
[15] A. Atmaca, R. Yumrutaş, Thermodynamic and exergoeconomic analysis of a cement plant: part II - Application, Energy Convers. Manag. 79 (2014) 799–808, doi: 10.1016/j.enconman.2013.11.054.
[16] E. Amiri Rad, S. Mohammadi, Energetic and exergetic optimized Rankine cycle for waste heat recovery in a cement factory, Appl. Therm. Eng. 132 (2018) 410–422, doi: 10.1016/j.applthermaleng.2017.12.076.
[17] E.P.B. Júnior, M.D.P. Arrieta, F.R.P. Arrieta, C.H.F. Silva, Assessment of a Kalina cycle for waste heat recovery in the cement industry, Appl. Therm. Eng. (2019), doi: 10.1016/j.applthermaleng.2018.10.088.
[18] J. Roy, M. Mishra, A. Misra, Parametric optimization and performance analysis of a waste heat recovery system using organic Rankine cycle, Energy 35 (12) (2010) 5049–5062, doi: 10.1016/j.energy.2010.08.013.
[19] S. Quoilin, S. Declaye, B.F. Tchanche, V. Lemort, Thermo-economic optimization of waste heat recovery organic Rankine cycles, Appl. Therm. Eng. 31 (14–15) (2011) 2885–2893, doi: 10.1016/j.applthermaleng.2011.05.014.
[20] Z. Shengjun, W. Huaixin, G. Tao, Performance comparison and parametric optimization of subcritical organic Rankine cycle (ORC) and transcritical power cycle system for low-temperature geothermal power generation, Appl. Energy 88 (8) (2011) 2740–2754, doi: 10.1016/j.apenergy.2011.02.034.
[21] C. He, C. Liu, H. Gao, H. Xie, Y. Li, S. Wu, J. Xu, The optimal evaporation temperature and working fluids for subcritical organic Rankine cycle, Energy 38 (1) (2012) 136–143, doi: 10.1016/j.energy.2011.12.022.
[22] F. Campana, M. Bianchi, L. Branchini, A. De Pascale, A. Peretto, M. Baresi, A. Fermi, N. Rossetti, R. Vescovo, ORC Waste heat recovery in European energy intensive industries: energy and GHG savings, Energy Convers. Manage. 76 (2013) 244–252, doi: 10.1016/j.enconman.2013.07.041.
[23] M. Imran, B.S. Park, H.J. Kim, D.H. Lee, M. Usman, M. Heo, Thermo-economic optimization of regenerative organic Rankine cycle for waste heat recovery applications, Energy Convers. Manage. 87 (2014) 107–118, doi: 10.1016/j.enconman.2014.06.091.
[24] S. Lecompte, S. Lemmens, H. Huisseune, M. van den Broek, M. De Paepe, Multi-Objective thermo-Economic optimization strategy for ORCs applied to subcritical and transcritical cycles for waste heat recovery, Energies 8 (4) (2015) 2714–2741, doi: 10.3390/en8042714.
[25] M. Yari, A.S. Mehr, V. Zare, S.M. Mahmoudi, M.A. Rosen, Exergoeconomic comparison of TLC (trilateral Rankine cycle), ORC (organic Rankine cycle) and kalina cycle using a low grade heat source, Energy 83 (2015) 712–722, doi: 10.1016/j.energy.2015.02.080.
[26] A. Bejan, G. Tsatsaronis, M. Moran, Thermal Design and Optimization, John Wiley & Sons, 1996.
[27] M. Imran, M. Usman, B.S. Park, Y. Yang, Comparative assessment of organic Rankine cycle integration for low temperature geothermal heat source applications, Energy 102 (2016) 473–490, doi: 10.1016/j.energy.2016.02.119.
[28] M. Kolahi, M. Yari, S.M. Mahmoudi, F. Mohammadkhani, Thermodynamic and economic performance improvement of ORCs through using zeotropic mixtures: case of waste heat recovery in an offshore platform, Case Stud. Therm. Eng. 8 (2016) 51–70, doi: 10.1016/j.csite.2016.05.001.
[29] Z. Han, P. Li, X. Han, Z. Mei, Z. Wang, Thermo-economic performance analysis of a regenerative superheating organic Rankine cycle for waste heat recovery, Energies 10 (10) (2017), doi: 10.3390/en10101593.
[30] A. Pantaleo, M. Simpson, G. Rotolo, E. Distaso, O. Oyewunmi, P. Sapin, P. De Palma, C. Markides, Thermoeconomic optimisation of small-scale organic Rankine cycle systems based on screw vs. piston expander maps in waste heat recovery applications, Energy Convers. Manag. 200 (2019) 112053, doi: 10.1016/j.enconman.2019.112053.
[31] L.M. van Kleef, O.A. Oyewunmi, C.N. Markides, Multi-objective thermo-economic optimization of organic Rankine cycle (ORC) power systems in waste-heat recovery applications using computer-aided molecular design techniques, Appl. Energy 251 (2019) 112513, doi: 10.1016/j.apenergy.2019.01.071.
[32] M. Bianchi, L. Branchini, A. De Pascale, F. Melino, A. Peretto, D. Archetti, F. Campana, T. Ferrari, N. Rossetti, Feasibility of ORC application in natural gas compressor stations, Energy 173 (2019) 1–15, doi: 10.1016/j.energy.2019.01.127.
[33] M. Feili, H. Ghaebi, T. Parikhani, H. Rostamzadeh, Exergoeconomic analysis and optimization of a new combined power and freshwater system driven by waste heat of a marine diesel engine, Therm. Sci. Eng. Progr. 18 (2020), doi: 10.1016/j.tsep.2020.100513.
[34] Y. Wang, Y. Liu, X. Liu, W. Zhang, P. Cui, M. Yu, Z. Liu, Z. Zhu, S. Yang, Advanced exergy and exergoeconomic analyses of a cascade absorption heat transformer for the recovery of low grade waste heat, Energy Convers. Manag. 205 (2020), doi: 10.1016/j.enconman.2019.112392.
[35] Z. Utlu, A. Hepbaşh, Exergoeconomic analysis of energy utilization of drying process in a ceramic production, Appl. Therm. Eng. 70 (1) (2014) 748–762, doi: 10.1016/j.applthermaleng.2014.05.070.
[36] U. National Minerals Information Center, Mineral Commodity Summaries, Technical Report, USGS, 2020, doi: 10.3133/mcs2020.
[37] DANE, Estadísticas de cemento gris (ECG) - 2019, Dane (2019) 1–29.
[38] A. Mahmoudi, M. Fazli, M.R. Morad, A recent review of waste heat recovery by organic Rankine cycle, Appl. Therm. Eng. (2018), doi: 10.1016/j.applthermaleng.2018.07.136.
[39] G. Shu, X. Li, H. Tian, X. Liang, H. Wei, X. Wang, Alkanes as working fluids for high-temperature exhaust heat recovery of diesel engine using organic Rankine cycle, Appl. Energy 119 (2014) 204–217, doi: 10.1016/j.apenergy.2013.12.056.
[40] S. Baral, D. Kim, E. Yun, K. Kim, Energy, exergy and performance analysis of small-Scale organic Rankine cycle systems for electrical power generation applicable in rural areas of developing countries, Energies 8 (2) (2015) 684–713, doi: 10.3390/en8020684.
[41] M.B. Moran, M.J. Shapiro, H.N. Boettner, D.D. Bailey, Fundamentals of Engineering Thermodynamics, 8th, John Wiley & Sons, Inc., 2014.
[42] K. M. N., W.D. Seider, D.R. Lewin, J.D. Seader, S. Widagdo, R. Gani, Product and process design principles: Synthesis, analysis and evaluation, 4th, John Wiley & Sons, Inc., 2019.
[43] E. Macchi, A. Perdichizzi, Efficiency prediction for axial-Flow turbines operating with nonconventional fluids., Am. Soc. Mech. Eng. (Paper) 103 (81 -GT-15) (1981) 5–11.
[44] I. Dincer, A. Sahin, A new model for thermodynamic analysis of a drying process, Int. J. Heat Mass Transf. 47 (4) (2004) 645–652, doi: 10.1016/j.ijheatmasstransfer.2003.08.013.
[45] R.E. PetersMax S; Timmerhaus, Klaus; West, Plant Design and Economics for Chemical Engineers, fifth, McGraw-Hill Education, 2003.
[46] J.R. Couper, W.R. Penney, J.R. Fair, S.M. Walas, Chemical Process Equipment: Selection and Design, third, Elsevier, 2012, doi: 10.1016/B978-0-12-396959-0.00025-2.
[47] C. Invernizzi, P. Iora, P. Silva, Bottoming micro-Rankine cycles for micro-gas turbines, Appl. Therm. Eng. 27 (1) (2007) 100–110, doi: 10.1016/j.applthermaleng.2006.05.003.